

Article

Correlation of the Growth Rate of the Hydrate Layer at a Guest/Liquid-Water Interface to Mass Transfer Resistance

Masatoshi Kishimoto and Ryo Ohmura *

Department of Mechanical Engineering, Keio University, 3-14-1 Hiyoshi, Kohoku-ku, Yokohama 223-8522, Japan; E-Mail: kishimasa1112@yahoo.co.jp

* Author to whom correspondence should be addressed; E-Mail: rohmura@mech.keio.ac.jp; Tel.: +81-45-566-1813; Fax: +81-45-566-1495.

Received: 14 December 2011; in revised form: 10 January 2012 / Accepted: 11 January 2012 /

Published: 18 January 2012

Abstract: Growth rate of a hydrate layer at the guest/liquid-water interface is analyzed considering the conjugate process of the mass-transfer and hydrate crystal growth. Hydrate-layer growth rate data in the literature are often compiled according to the system subcooling ($\Delta T \equiv T_{\text{eq}} - T_{\text{ex}}$, where T_{eq} is the equilibrium dissociation temperature of the hydrate and T_{ex} is the system temperature), suggesting predominant heat transfer limitations. In this paper, we investigate how the existing data on hydrate-layer growth is better correlated to mass transfer of the guest species in liquid water in three-phase equilibrium with bulk guest fluid and hydrate. We have analyzed the conjugate processes of mass-transfer/hydrate-layer-growth following our previous study on the hydrate crystal growth into liquid water saturated with a guest substance. A dimensionless parameter representing the hydrate-layer growth rate is derived from the analysis. This analysis is based on the idea that the growth rate is controlled by the mass transfer of the hydrate-guest substance, dissolved in the bulk of liquid water, to the front of the growing hydrate-layer along the guest/water interface. The variations in the hydrate-layer growth rate observed in the previous studies are related to the dimensionless parameter.

Keywords: clathrate hydrate; crystal growth rate; mass transfer

1. Introduction

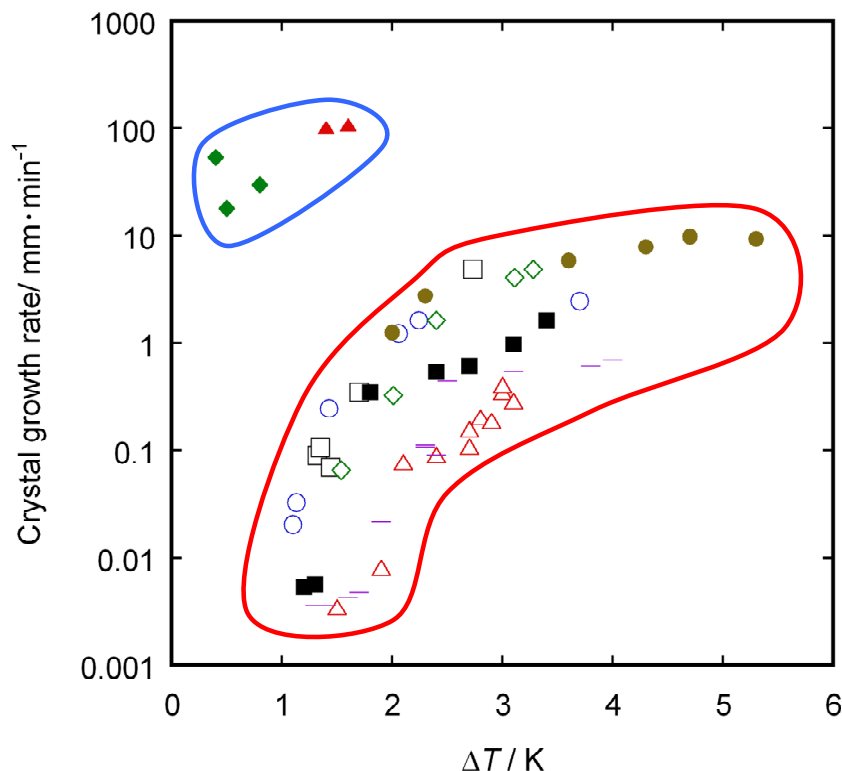
Clathrate hydrates are crystalline solid compounds consisting of hydrogen-bond water molecules forming cages that enclose other small molecules. Clathrate hydrates have several unique properties, such as a large heat of formation/decomposition, guest-substance selectivity, and a high gas storage capacity. Recently, research and development of novel energy-environment-related technologies, exploiting these properties and characteristics of hydrates are being performed. Some of these novel technologies are transportation and storage of natural gases [1] and hydrogen [2], ground/ocean sequestration of carbon dioxide [3–5], development of heat pump/refrigeration systems [6], removal of hydrogen sulfide from biogas [7], isolation of greenhouse gases [8], etc. Investigations of the dominant factors in the formation and growth of clathrate hydrates have long been of scientific and industrial interest. Despite the fact that our understanding of hydrate formation from guest-water solutions has improved [9–11], much discussion still exists in the literature [12–17] about the dominant process controlling the hydrate-layer growth along the guest/liquid-water interface. Some previous studies [12–14] have suggested that the hydrate-layer growth is significantly affected by heat transfer. If the heat-transfer is the controlling process, the rate of hydrate-layer growth should be dependent on the subcooling (ΔT) of the system. The subcooling (ΔT) is the deficiency of the system temperature from the hydrate equilibrium temperature ($\Delta T \equiv T_{eq} - T_{ex}$) as the index of the driving force for the crystal growth, where T_{eq} is the equilibrium temperature of the hydrate and T_{ex} is the system temperature.

Figure 1 shows the compiled data from the literature for the hydrate-layer growth rate based on the reported subcooling (ΔT) in the system. As seen in the figure, there is a significant scatter of the growth rate data. Particularly, the growth rate of CO₂ hydrate is greater by 1–2 orders of magnitude than those of methane and propane hydrates. If heat transfer were the dominant controlling process for hydrate-layer growth, there should be a good correlation between the data and ΔT .

Pointing out that the correlation between the experimentally-measured rate data and ΔT is not necessarily good, Saito *et al.* examined whether the hydrate-layer growth can, instead, be correlated to mass transfer effects at the guest/liquid-water interface [18]. In their study, they simply attempted to correlate the rate data to the concentration difference (Δx_g) representing the driving force for the mass transfer of a guest substance in liquid water [18]. They obtained the better correlation using the concentration difference. However, the analysis can be improved in that the effect of composition of hydrates to the hydrate growth rate was not considered, and hence, there is still a room for further study.

In the present study, we first present the theoretical formulations representing the conjugate process of guest-in-water mass transfer and the hydrate-layer growth following to the previous study on the hydrate crystal growth into the liquid water saturated with a guest substance prior to the hydrate formation [15]. We have derived a dimensionless parameter representing the hydrate-layer growth rate. This analysis is based on the idea that the growth rate is controlled by the mass transfer of the hydrate-guest substance, dissolved in the bulk of liquid water, to the front of the growing hydrate-layer along the guest-water interface.

Figure 1. Dependence of hydrate-layer growth rate on the subcooling ΔT for several reported studies: (□) methane at 5.60 MPa [12]; (○) methane at 8.15 MPa [12]; (◇) methane at 10.56 MPa [12]; (△) propane at 0.31 MPa [12]; (—) propane at 0.41 MPa [12]; (■) propane at 0.51 MPa [12]; (●) methane [13]; (◆) CO₂(vapor) at 3 MPa [14]; (▲) CO₂(gas) at 5 MPa [14].



2. Formulations for the Conjugate Process of Mass Transfer and Hydrate Crystal Growth

Figure 2 illustrates the hydrate layer growing at the guest/liquid-water interface and represents the physical model of the analysis. Here, we assume that a local three-phase equilibrium exists at the front of the hydrate-layer growing at the guest/liquid-water interface. The driving force, Δx_g , is the difference between the solubility of the guest ($x_{eq,int}$) in liquid-water at the guest/liquid-water interface at the system temperature (T_{ex}) and the solubility of the guest ($x_{eq,hyd}$) in liquid/water at the hydrate equilibrium temperature (T_{eq}) at the hydrate-layer front, $\Delta x_g \equiv x_{eq,int} - x_{eq,hyd}$.

Figure 2. Illustration of hydrate-layer growth at the guest/liquid-water interface.

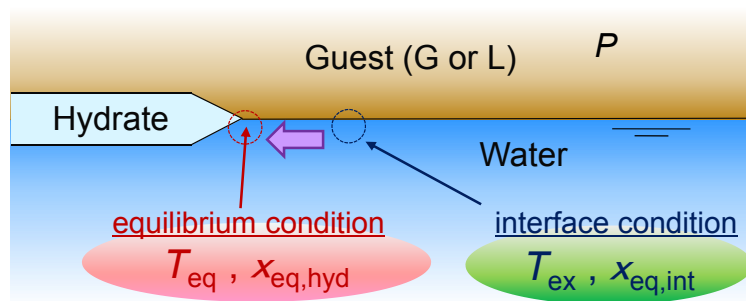
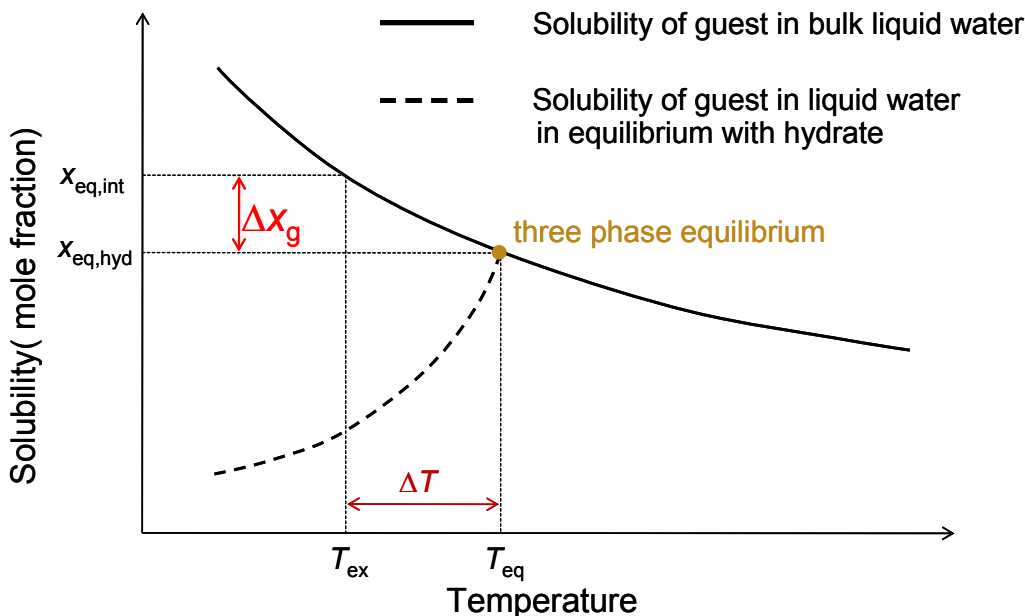


Figure 3 shows a schematic of the solubility for the guest in liquid-water as a function of the temperature. The solid line corresponds to the two-phase equilibrium conditions with the solubility of the guest in bulk liquid-water, and the dashed line is the equilibrium solubility of the guest in liquid-water in equilibrium with the hydrate. The intersection of the lines indicates the liquid-water-hydrate-guest phase equilibrium condition at the equilibrium temperature T_{eq} under the experimental pressure. The solubility $x_{eq,int}$ corresponds to the experimental system temperature T_{ex} .

Figure 3. Schematic of solubility curves of guest species in liquid-water.



As for the mathematical formulation of the conjugate process, we may follow on the previous study by Ohmura *et al.* [15] on the hydrate crystal growth into the liquid-water. A similar analysis to the hydrate crystal growth at guest/liquid-water interface was performed.

At first, we consider the molar flux \dot{m}_g of a guest substance supplied to the surface of a hydrate crystal. As this flux is caused by the diffusive, or convective, mass transfer of the guest substance from guest/liquid-water interface to the crystal surface, it may be expressed as:

$$\dot{m}_g = h_{m,g} \rho_l [x_{eq,int} - x_{eq,hyd}] = h_{m,g} \rho_l \Delta x_g \quad (1)$$

where $h_{m,g}$ is the mass transfer coefficient for the guest substance, ρ_l is the molar density of liquid water. The molar flux \dot{m}_g of the guest substance at the crystal surface should induce a volumetric growth rate \dot{V}_h of the crystal per its unit surface area, which may be evaluated as:

$$\dot{V}_h = \frac{\dot{m}_g (M_g - n M_w)}{\rho_h} \quad (2)$$

where M_g and M_w are the molar masses of the guest substance and water, respectively, n is the hydration number, the ratio of the number of water molecules to that of guest molecules in the hydrate, and ρ_h is the mass density of the hydrate.

The subject of the formulations is then to find how to express \dot{V}_h in terms of the parameters that we can evaluate a priori and to correlate \dot{V}_h to a group of such parameters. This is described below.

The density ρ_h of the hydrate used in Equation (2) is given by:

$$\rho_h = \frac{(N_w/n)(M_g + nM_w)}{Aa^3} \quad (3)$$

where A is the Avogadro number, N_w is the number of water molecules in each unit cell of the hydrate and a is the lattice constant for the hydrate. Substituting Equations (1) and (3) into Equation (2), we obtain:

$$\dot{V}_h = h_{m,g} \rho_l A \frac{a^3}{N_w} n \Delta x_g \quad (4a)$$

If we approximate ρ_l by ρ_w , the molar density of pure water, Equation (4a) is modified as follows:

$$\dot{V}_h = h_{m,g} \left(\frac{a^3 \rho_w A}{N_w} \right) n \Delta x_g \quad (4b)$$

where the dimensionless group in the parentheses on the right-hand side of Equation (4b) expresses the ratio of the volume a^3/N_w per one water molecule in each unit cell of the hydrate, to the molecular volume of water in its liquid state. Whether the hydrate of interest is of structure I ($a = \sim 1.2$ nm; $N_w = 46$) or of structure II ($a = \sim 1.73$ nm; $N_w = 136$), the value of the above dimensionless group is evaluated to be 1.25 to 1.27. We can assume this to be a constant common to all structure I and structure II forming guest substances only weakly soluble in liquid water. Consequently, Equation (4b) may be simplified as:

$$\dot{V}_h \propto h_{m,g} n \Delta x_g \quad (5)$$

It is quite difficult to evaluate $h_{m,g}$ in actual hydrate-forming experimental systems because $h_{m,g}$ should depend on various factors, including free convection induced in liquid water due to spatial variations in temperature and/or guest in water concentration. As a first approximation, we assume here that $h_{m,g}$ is simply proportional to $D_{g,w}$, the diffusion coefficient of the guest substance in liquid-water. Thus, we have the following relation:

$$\dot{V}_h \propto D_{g,w} n \Delta x_g \quad (6)$$

The values of $D_{g,w}$ for the guest substances are presumed to be similar to each other. We can estimate these values for methane, carbon dioxide and propane, to be about $1 \times 10^{-9} \text{ m}^2 \cdot \text{s}^{-1}$ by using the Wilke-Change Equation [19], incorporating an association-parameter value recommended by Hayduk and Laudie [20]. The above variation in $D_{g,w}$ is insignificant compared with that in $x_{eq,int}$ and $x_{eq,hyd}$ which varies by a factor of about 100. Therefore, we may assume the very simple relation for crystal-layer growth as follows:

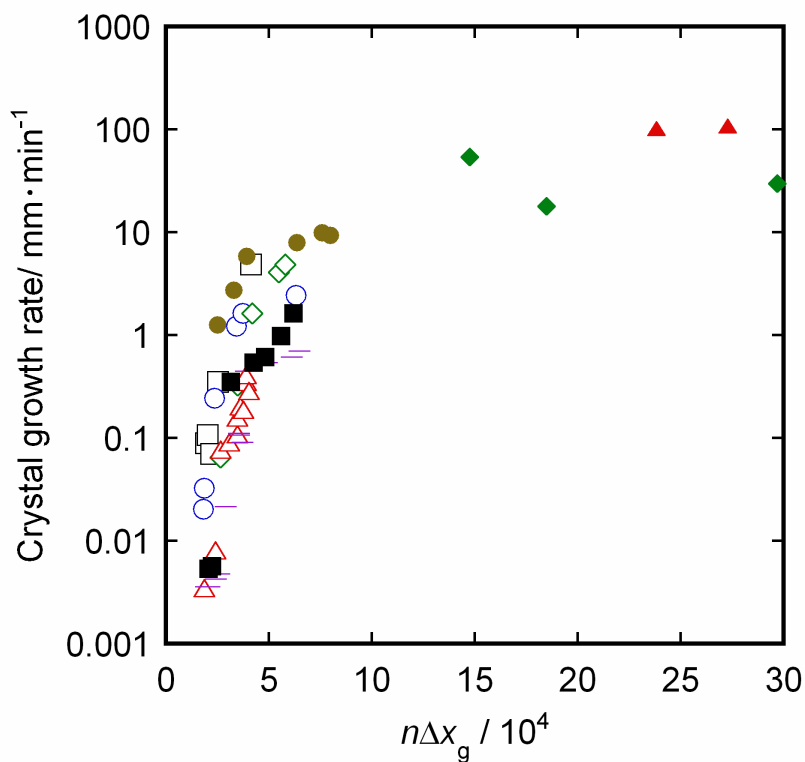
$$\dot{V}_h \propto n \Delta x_g \quad (7)$$

3. Results and Discussion

Based on the analysis in the previous section, the data of the hydrate-layer growth rates for the systems in Figure 1 were re-plotted in Figure 4 with $n \Delta x_g$ as an index for the effective driving force of

the volumetric hydrate growth. In numerically evaluating the values of $n\Delta x_g$, the guest-in-water solubility $x_{eq,int}$ and $x_{eq,hyd}$ were calculated with a phase equilibrium calculation program, HWHydrateGUI [21]. The deviations of the predictions with HWHydrate from the existing experimental data [22–25] are calculated to be mostly within $\pm 5\%$, and at worst within $\pm 15\%$ over the pressure-temperature range corresponding to the experimental measurements of hydrate-layer growth rates, specifically pressures from 3.5 to 10.5 MPa, temperatures from 274 to 283 K for methane, 0.3 to 0.5 MPa, 273 to 277 K for propane, and 3 to 5 MPa, 274 to 280 K for CO₂. The hydration numbers n for methane, CO₂ and propane are evaluated to be 6, 6.2 and 17 respectively, by referring to the direct measurements of the hydrate compositions by Raman spectroscopy for methane hydrate [26,27], by means of single-crystal X-ray diffraction for CO₂ hydrate [28], and by assuming that propane molecules occupy only the large cages in the structure-II hydrate [29].

Figure 4. Dependence of hydrate-layer growth rate on the $n\Delta x_g$ for the systems in Figure 1: (□) methane at 5.60 MPa [12]; (○) methane at 8.15 MPa [12]; (\diamond) methane at 10.56 MPa [12]; (\triangle) propane at 0.31 MPa [12]; (—) propane at 0.41 MPa [12]; (■) propane at 0.51 MPa [12]; (●) methane [13]; (◆) CO₂(vapor) at 3 MPa [14]; (\blacktriangle) CO₂(gas) at 5 MPa [14].



Comparison of Figures 1 to 4 indicates that the hydrate-layer growth rate data are better correlated with $n\Delta x_g$ than with ΔT , *i.e.*, the mass transfer of the guest species in liquid water may have a significant effect on the hydrate-layer growth at the guest/liquid-water interface, as opposed to heat transfer limitations alone. The implication of this analysis is that the studies of hydrate growth kinetics must carefully consider both the heat and mass transfer processes and not only either heat or mass transfer in the design and analysis of experimental measurements.

4. Conclusions

We have investigated the correlation between the growth rate of the hydrate layer at a guest/liquid water interface to the resistance of mass transfer of the guest species dissolved in liquid water. Based on the idea that the growth rate is controlled by the mass transfer of the guest substance dissolved in the bulk of liquid water, to the front of the growing hydrate-layer along the guest/water interface, the conjugate processes of mass-transfer and hydrate-layer growth are formulated. From this formulating analysis, a dimensionless parameter representing the hydrate-layer growth rate is derived. The variations in the hydrate-layer growth rate experimentally measured in previous studies are well correlated to this dimensionless parameter, thereby indicating the significant effect of mass transfer to the hydrate-layer growth.

Acknowledgments

This study was supported by a Grant-in-Aid for Science Research from the Japan Society for the Promotion of Science (Grant 22760157) and by a Grant-in-Aid for the Global Center of Excellent Program for “Center for Education and Research of Symbiotic, Safe and Secure System Design” from the Ministry of Education, Culture, Sport, and Technology in Japan.

References

1. Mori, Y.H. Recent advances in hydrate-based technologies for natural gas storage—A review. *J. Chem. Ind. Eng. (China)* **2003**, *54*, 1–17.
2. Mao, W.L.; Mao, H. Hydrogen storage in molecular compounds. *Proc. Natl. Acad. Sci. USA* **2004**, *101*, 708–710.
3. Ohmura, R.; Mori, Y.H. Critical conditions for CO₂ hydrate films to rest on submarine CO₂ pond surfaces: A mechanistic study. *Environ. Sci. Technol.* **1998**, *32*, 1120–1127.
4. Brewer, P.G.; Peltzer, E.; Aya, I.; Haugan, P.; Bellerby, R.; Yaname, K.; Kojima, R.; Waltz, P.; Nakajima, Y.J. Small scale field study of an ocean CO₂ plume. *J. Oceanogr.* **2004**, *60*, 751–758.
5. Brewer, P.G.; Frienderich, G.; Petlter, E.T.; Orr, F.M., Jr. Direct experiments on the ocean disposal of fossil fuel CO₂. *Science* **1999**, *284*, 943–945.
6. Ogawa, T.; Ito, T.; Watanabe, K.; Tahara, K.; Hiraoka, R.; Ochiai, J.; Ohmura, R.; Mori, Y.H. Development of a novel hydrate-based refrigeration system: A preliminary overview. *Appl. Therm. Eng.* **2006**, *26*, 2157–2167.
7. Kamata, Y.; Yamakoshi, Y.; Ebinuma, T.; Oyama, H.; Shimada, W.; Narita, H. Hydrogen sulfide separation using Tetra-*n*-butyl ammonium bromide semi-clathrate (TBAB) hydrate. *Energy Fuels* **2005**, *19*, 1717–1722.
8. Seo, Y.-T.; Moudravski, I.L.; Ripmeester, J.A.; Lee, J.-W.; Lee, H. Efficient recovery of CO₂ from flue gas by clathrate hydrate formation in porous silica gels. *Environ. Sci. Technol.* **2005**, *39*, 2315–2319.
9. Nagashima, K.; Yamamoto, Y.; Takahashi, M.; Komai, T. Interferometric observation of mass transport processes adjacent to tetrahydrofuran clathrate hydrates under nonequilibrium conditions. *Fluid Phase Equilib.* **2003**, *214*, 11–24.

10. Sabase, Y.; Nagashima, K. Growth mode transition of tetrahydrofuran clathrate hydrates in the guest/host concentration boundary layer. *J. Phys. Chem. B* **2009**, *113*, 15304–15311.
11. Iida, T.; Mori, H.; Mochizuki, T.; Mori, Y.H. Formation and dissociation of clathrate hydrate in stoichiometric tetrahydrofuran–water mixture subjected to one-dimensional cooling or heating. *Chem. Eng. Sci.* **2001**, *56*, 4747–4758.
12. Tanaka, R.; Sakemoto, R.; Ohmura, R. Crystal growth of clathrate hydrates formed at the interface of liquid water and gaseous methane, ethane, or propane: Variations in crystal morphology. *Cryst. Growth Des.* **2009**, *9*, 2529–2536.
13. Freer, E.M.; Selim, M.S.; Sloan, E.D. Methane hydrate film growth kinetics. *Fluid Phase Equilib.* **2001**, *185*, 65–75.
14. Uchida, T.; Ebinuma, T.; Kawabata, J.; Narita, H. Microscopic observations of formation processes of clathrate-hydrate films at an interface between water and carbon dioxide. *J. Cryst. Growth* **1999**, *204*, 348–356.
15. Ohmura, R.; Shimada, W.; Uchida, T.; Mori, Y.H.; Takya, S.; Nagao, J.; Minagawa, H.; Ebinuma, T.; Narita, H. Clathrate hydrate crystal growth in liquid water saturated with a hydrate-forming substance: variations in crystal morphology. *Philos. Mag.* **2004**, *84*, 1–16.
16. Taylor, C.J.; Miller, K.T.; Koh, A.; Sloan, E.D. Macroscopic investigation of hydrate film growth at the hydrocarbon/water interface. *Chem. Eng. Sci.* **2007**, *62*, 6542–6533.
17. Peng, B.Z.; Dandekar, A.; Sun, C.Y.; Ma, Q.L.; Pang, W.X.; Chen, G.J. Hydrate film growth on the surface of a gas bubble suspended in water. *J. Phys. Chem. B* **2007**, *111*, 12485–12493.
18. Saito, K.; Sum, A.K.; Ohmura, R. Correlation of hydrate-film growth rate at the guest/liquid-water interface to mass transfer resistance. *Ind. Eng. Chem. Res.* **2010**, *49*, 7102–7103.
19. Wilke, C.R.; Chang, P. Correlation of diffusion coefficients in dilute solutions. *AIChE J.* **1955**, *1*, 264–270.
20. Hyduk, W.; Laudie, H. Prediction of diffusion coefficients for nonelectrolytes in dilute aqueous solutions. *AIChE J.* **1974**, *20*, 611–615.
21. HWHydrateGUI (version 1.1). Phase-equilibrium calculation program developed at the Centre for Gas Hydrate Research, Heriot-Watt University, Edinburgh, UK, 2005.
22. Dodds, W.S.; Stutzman, L.F.; Sollami, B.J. Carbon dioxide solubility in water. *Ind. Eng. Chem., Chem. Eng. Data Ser.* **1956**, *1*, 92–95.
23. Lekvam, K.; Bishnoi, P.R. Dissolution of methane in water at low temperature and intermediate pressures. *Fluid Phase Equilib.* **1997**, *131*, 297–309.
24. Servio, P.; Englezos, P. Measurement of dissolved methane in water in equilibrium with its hydrate. *J. Chem. Eng.* **2002**, *47*, 87–90.
25. Gaudette, J.; Servio, P. Measurement of dissolved propane in water in the presence of gas hydrate. *J. Chem. Eng. Data* **2007**, *52*, 1449–1451.
26. Sum, A.K.; Burruss, R.C.; Sloan, E.D. Measurement of clathrate hydrates via raman spectroscopy. *J. Phys. Chem. B* **1997**, *101*, 7371–7377.
27. Uchida, T.; Hirano, T.; Ebinuma, T.; Narita, H.; Gohara, K.; Mae, S.; Matsumoto, R. Raman spectroscopic determination of hydration number of methane hydrates. *AIChE J.* **1999**, *45*, 2641–2645.

28. Udachin, K.A.; Ratcliffe, C.I.; Ripmeester, J.A. Structure, composition, and thermal expansion of CO₂ hydrate from single crystal X-ray diffraction measurements. *J. Phys. Chem. B* **2001**, *105*, 4200–4204.
29. Brouwer, D.H.; Brouwer, E.B.; Maclaurin, G.; Lee, M.; Parks, D.; Ripmeester, J.A. Some new halogen-containing hydrate-formers for structure I and II clathrate hydrates. *Supramolec. Chem.* **1997**, *8*, 361–367.

© 2012 by the authors; licensee MDPI, Basel, Switzerland. This article is an open access article distributed under the terms and conditions of the Creative Commons Attribution license (<http://creativecommons.org/licenses/by/3.0/>).